

# Analysis and Mitigation of Shared Resource Contention on Heterogeneous Multicore: An Industrial Case Study

Michael Bechtel, Heechul Yun  
University of Kansas, USA.  
{mbechtel, heechul.yun}@ku.edu

**Abstract**—In this paper, we present a solution to the industrial challenge put forth by ARM in 2022. We systematically analyze the effect of shared resource contention to an augmented reality head-up display (AR-HUD) case-study application of the industrial challenge on a heterogeneous multicore platform, NVIDIA Jetson Nano. We configure the AR-HUD application such that it can process incoming image frames in real-time at 20Hz on the platform. We use Microarchitectural Denial-of-Service (DoS) attacks as aggressor workloads of the challenge and show that they can dramatically impact the latency and accuracy of the AR-HUD application. This results in significant deviations of the estimated trajectories from known ground truths, despite our best effort to mitigate their influence by using cache partitioning and real-time scheduling of the AR-HUD application. To address the challenge, we propose RT-Gang++, a partitioned real-time gang scheduling framework with LLC and iGPU bandwidth throttling capabilities. By applying RT-Gang++, we are able to achieve desired level of performance of the AR-HUD application even in the presence of fully loaded aggressor tasks.

**Index Terms**—Industrial Challenge, Real Time, SLAM, Microarchitectural DoS Attack

## I. INTRODUCTION

Heterogeneous multicore computing platforms are increasingly utilized in safety-critical cyber physical systems (CPS) as they can offer significant performance improvements while simultaneously meeting size, weight, and power (SWaP) constraints. However, contention on shared microarchitectural resources, such as shared cache and main memory, between the computing elements in such a platform remains a significant challenge because it can impact the execution timings of critical real-time tasks and thus jeopardize the safety of the CPS. Moreover, shared resource contention can also be intentionally induced by malicious actors with the goal of compromising the performance and safety of CPS. Such adversaries are known as microarchitectural Denial-of-Service (DoS) attacks [9], and are especially problematic for high-performance CPS that need to run multiple concurrent applications simultaneously on a single multicore platform. Given the recent trends towards connected CPS, as can be seen in ARM’s SOAFEE initiative [4] for the automotive industry, it is conceivable that such DoS attacks could be remotely deployed on future CPS.

Understanding and addressing shared resource contention in multicore has been of intense interest for both academia and industry in recent years. In particular, ARM issued an

Industrial Challenge in 2022 to address the problem of shared resource contention [3]. The challenge is centered around an augmented reality head-up display (AR-HUD) case-study for automotive applications. The case-study application is composed of two main components: a Visual Simultaneous Localization and Mapping (SLAM) task [14] and a DNN-based driver head pose estimation task [15]. The SLAM task is composed of three main threads, all of which run on the CPU, whereas the DNN-based head-pose estimation task (we henceforth refer it as the DNN task) may utilize the GPU. The application represents a computationally intensive mixed-criticality real-time system that must leverage high-performance heterogeneous multicore embedded platforms. As such, the challenge seeks to find ways to analyze and optimize performance bounds of such critical real-time tasks even in the presence of “aggressor tasks”, which may contend with the critical real-time task in accessing shared resources.

In this paper, we first study the impact of shared resource contention to the performance of the AR-HUD case-study application of ARM’s Industrial Challenge. Through our study, we aim to answer the following questions: (1) Can we safely consolidate the two real-time tasks (the SLAM algorithm and head pose detection) in the AR-HUD case-study on a representative heterogeneous system-on-chip (SoC) processor and achieve good real-time performance? (2) Does shared resource contention between the two AR-HUD tasks impact the accuracy of the obtained position/trajectory estimates of the SLAM task? (3) Can we guarantee a desired level of performance, in terms of both accuracy and latency, of the AR-HUD application in the presence of aggressor tasks—which may be maliciously designed to cause high shared resource contention—without excessive over-provisioning?

To answer these questions, we systematically conduct experiments on an NVIDIA Jetson Nano, a representative heterogeneous embedded multicore platform that features a quad-core ARM Cortex-A57 CPU and an integrated GPU. Our findings are as follows: We are able to configure the AR-HUD application such that it can process incoming image frames in real-time at 20Hz. However, we find that contention between the two real-time tasks does significantly impact the accuracy of the SLAM task, which results in significant deviations of the estimated trajectories from the ground truth even when it

could process all input image frames in real-time at 20Hz. In addition, we find that cache bank-aware DoS attack [7] is especially effective in impacting the accuracy and real-time performance of the AR-HUD application. Concretely, when the cache bank-aware DoS attack tasks are co-scheduled as best-effort (non-RT) tasks together of the real-time tasks of the AR-HUD application to fully load the system, the SLAM task fails to even generate the trajectory as it has to drop most of the incoming image frames due to increased latency caused by contention.

To address the challenge, we propose RT-Gang++, a partitioned real-time gang scheduling framework with iGPU and last level cache (LLC) bandwidth throttling capabilities. RT-Gang++ is based on [2] but extends its capabilities as follows: (1) add support for partitioned gang-scheduling to allow for multiple real-time gangs of different priorities to execute concurrently; (2) add support for LLC and iGPU bandwidth throttling to protect against contention on those shared resources. These additional capabilities are crucial to address the ARM industrial challenge problem. By employing RT-Gang++, we are able to safely consolidate the AR-HUD application, even in the presence of malicious DoS attacks, and achieve desired real-time performance and accuracy.

This paper makes the following **contributions**:

- We systematically study the effect of shared resource contention on the performance of the AR-HUD application, using state-of-the-art denial-of-service (DoS) attackers as additional aggressor tasks [9]. We find the recently proposed cache bank-aware DoS attack [7] to be especially effective in delaying the execution latency and, consequently, degrading the accuracy of the SLAM algorithm. We also find that executing GPU kernels can significantly impact the performance of the SLAM algorithm, which runs on the CPU.
- We show that the SLAM algorithm’s accuracy can degrade even when input frames are processed in real-time (i.e., meeting their deadline) because the increased execution latency of the SLAM task’s key threads can significantly impact the accuracy. We find that these delays cause the trajectory generated by the SLAM algorithm to significantly deviate from the ground truth.
- We propose RT-Gang++, an extension to the RT-Gang scheduling framework that enables partitioned gang scheduling, LLC and iGPU bandwidth throttling capabilities to better protect diverse real-time tasksets. By employing RT-Gang++, we show that it can effectively protect the performance of the AR-HUD application even in the presence of aggressor tasks without over-provisioning the system. Note that RT-Gang++ will be released as open-source.

The rest of this paper is organized as follows. Section II describes the ARM Industrial Challenge problem. Section III describes microarchitectural DoS attacks for the challenge. Section IV discusses our experimental setup. Section V presents our empirical evaluation of the challenge’s case-study

application. Section VI presents a mitigation approach and its effects. We review related work in Section VII and conclude in Section VIII.

## II. ARM INDUSTRIAL CHALLENGE 2022: AUGMENTED REALITY HEAD-UP DISPLAY (AR-HUD) APPLICATION

Addressing the impacts of shared resource contention is of critical importance for many high-performance CPS, such as those in the robotics and automotive fields. This is especially the case given the increased importance of consolidating high-performance mixed criticality applications in CPS. To stimulate further research on this topic, ARM introduced an Industrial Challenge in ECRTS 2022. The challenge presented an augmented reality head-up display (AR-HUD) application in the automotive context as a case-study. As an advanced driver assistance system (ADAS), this application provides additional alerts and notifications to the driver of a vehicle in real-time. In particular, these alerts are overlaid on real-world objects using augmented reality (AR) technology. For the suggested AR-HUD application, it is mainly comprised of two components: a Visual SLAM task, and a head pose estimation task. We now briefly introduce and discuss both AR-HUD components.

For many autonomous cyber physical systems (CPS), localization and 3D map generation are important steps for real-world performance. Increasingly, many CPS employ Simultaneous Localization and Mapping (SLAM) algorithms to perform both operations in a single step. In a SLAM algorithm, input sensor data is received and utilized to both estimate a system’s current position in, and generate/update a 3D map of a given environment. Vision (camera) and range sensors such as LIDARs, lasers and sonars can be used for SLAM. The category of SLAM algorithms that utilize vision has come to be known as *Visual SLAM*.

In the ARM industrial challenge, the  $OV^2$ SLAM algorithm [14] is suggested as part of the AR-HUD case study [3].  $OV^2$ SLAM is a Visual SLAM algorithm that is geared towards real-time applications and emphasizes processing time in addition to SLAM performance. It is composed of four main components with each one being assigned to a separate thread:

- 1) The *Front-End* thread performs real-time pose estimation of the camera sensor. It is also responsible for creating the keyframes used to generate 3D maps of surrounding environments. Note that this thread runs for every input frame that is received, meaning that it is a periodic task in nature. For our purposes, we target a per-frame deadline of 50 ms as the input datasets we use in our evaluations playback data at a frequency of 20 Hz.
- 2) The *Mapping* thread uses keyframes generated in the *Front-End* to generate new 3D map points. It primarily does this by performing triangulation on the keyframes. Then, if a new keyframe has not arrived, it will also perform local map tracking in order to minimize drift. Unlike the *Front-End*, the *Mapping* thread is aperiodic

as it is event-driven and only runs when a new keyframe is generated.

- 3) The *State Optimization* thread performs two main operations. First, it runs a local bundle adjustment (BA) to refine camera pose estimations. Second, it runs a keyframe filtering pass that prevents redundant keyframes from being processed in future BA operations. Note that this thread is also aperiodic as it relies on input from the *Mapping* thread, meaning that it is also event-driven.
- 4) The *Loop Closer* thread performs an online bag-of-words (BoW) operation to detect loop closures in a system’s given trajectory. However, we do not employ this thread in our case study as it is not necessary for the target AR-HUD application [3].

Note that only the *Front-End* thread runs for every input frame that is fed to OV<sup>2</sup>SLAM. The remaining threads will then only run when necessary, such as when a new keyframe is created.

By default, the OV<sup>2</sup>SLAM algorithm can be run in one of three different modes: *accurate*, *fast*, and *average*. The *accurate* mode of operation performs all four steps described above, including Loop Closure, and is intended to maximize accuracy while still maintaining a control frequency of 20 Hz. On the other hand, the *fast* mode of operation instead sacrifices some accuracy so that it can operate at a much faster 200 Hz control frequency. To achieve this, the *fast* version uses a faster (but less accurate) keypoint detection algorithm and does not perform the Loop Closure step. The *average* version then operates in between the other two versions performance-wise. In other words, it runs at a control frequency between 20 and 200 Hz, and achieves accuracy worse than the *accurate* version but better than the *fast* version. Like the *accurate* version, though, the *average* version also performs Loop Closure. The Industrial Challenge suggests to use the *fast* version for its superior real-time performance and good accuracy.

For the AR-HUD application, it is also important that the ADAS alerts provided to the driver are displayed in a way that matches the driver’s viewpoint. To achieve this, the head pose of the driver can be estimated so that the AR display can be corrected as necessary. As such, the AR-HUD application employs a head pose estimation task for its second component. The Industrial Challenge suggests to use the HopeNet-Lite head pose estimator [15], as it can run in real-time on many embedded heterogeneous multicore platforms. We further discuss this component in our evaluation setup.

### III. MICROARCHITECTURAL DENIAL-OF-SERVICE (DOS) ATTACKS

As part of the Industrial Challenge, ARM also envisioned the presence of *aggressor workloads* in the AR-HUD case study [3]. These aggressor workloads may be co-scheduled alongside the AR-HUD application and may contend for shared resources.

For our aggressor workloads, we employ microarchitectural denial-of-service (DoS) attacks that have been described in literature [38], [9], [7]. These DoS attacks target various

microarchitectural resources in multicore platforms (e.g. LLC, DRAM) and can cause significant execution time delays to cross-core real-time tasks, even if they run on dedicated cores and have dedicated LLC partitions. In this work, we want to know the impacts such DoS attacks can have on the AR-HUD application. The specific DoS attacks we employ in our evaluations are as follows:

- The *bandwidth* benchmark from the IsolBench suite [38]. This benchmark is designed to perform continuous accesses to a target shared resource (e.g. LLC or DRAM) in a sequential manner. To be more specific, it performs sequential accesses over a 1D array at a cache line granularity (i.e. all accesses are 64B apart). We refer to DoS attacks based on this benchmark as *Bw*.
- The *latency-mlp* benchmark from the IsolBench suite [38]. Much like the *bandwidth* benchmark, *latency-mlp* continually accesses a target resource but differs in its access pattern due to its pointer chasing nature. Namely, it performs random accesses over multiple parallel linked lists (PLL). We refer to DoS attacks based on this benchmark as *PLL*.
- The cache bank-aware attacks from [7]. Much like memory-aware attacks [6], these attacks are based on the *PLL* attacks above but are modified to only access a specific cache bank in order to generate maximum cache bank contention in accessing the LLC. We refer to this attack as *BkPLL*.

Furthermore, these DoS attacks can be configured in two additional facets. First, they can all be configured to perform either read or write accesses. As such, we test DoS attacks of both access variations in our testing. Second, as mentioned above, the attackers can be configured to access the LLC or DRAM, so we employ separate DoS attacks targeting each shared resource. Note that we configure the *BkPLL* attacks to only access the LLC, as they are specifically designed for that resource. Putting it altogether notation wise, we use the following naming convention for DoS attacks:

$\langle DoS\ attack\ type \rangle \langle access\ type \rangle \langle target\ resource \rangle$

Where *DoS attack type* is one of the attacks from the above list, the *access type* is either read or write, and the *target resource* is either the LLC or DRAM. For example, an instance of the *Bw* attack that performs read accesses targeted to the LLC would be referred to as *BwRead(LLC)*. In total, we employ 10 different DoS attacker tasks in our evaluation.

### IV. EXPERIMENT SETUP

In this section, we describe the experimental setup for our case study of the AR-HUD application.

#### A. Hardware Platform

We deploy all target applications and DoS attacker tasks on an ARM-based Nvidia Jetson Nano embedded platform. The Jetson Nano equips a quad-core cluster of Cortex-A57 cores, with each core having its own private L1 instruction and data caches and all cores sharing access to a global L2

cache. Table I shows the basic characteristics of the Jetson Nano platform.

Platform	Nvidia Jetson Nano
SoC	Tegra X1
CPU	4x Cortex-A57 @ 1.43GHz
GPU	128-core Maxwell
Shared LLC (L2)	2MB (16-way)
Memory (Peak B/W)	4GB LPDDR4 (25.6 GB/s)

TABLE I: Nvidia Jetson Nano hardware specifications.

### B. Application Setup

As discussed in Section II, the AR-HUD application is comprised of two main components: the OV<sup>2</sup>SLAM Visual SLAM task, and the HopeNet-Lite head pose estimation task.

For the SLAM task, we use the *fast* setting of OV<sup>2</sup>SLAM, as recommended in the Industrial Challenge [3], which is comprised of three threads: *Front End*, *Mapping*, and *State Optimization*. The *Front End* thread is invoked whenever the camera provides a new image frame, which in our case is at a fixed rate of 20Hz. The *Mapping* and *State Optimization* threads are invoked conditionally when the *Front End* thread decides to generate a new key frame (See II for more details). As the SLAM task is *real-time critical* [3], we use the Linux SCHED\_FIFO real-time scheduler and assign it a real-time priority of 2. Furthermore, we assign all three threads of the SLAM task onto two CPU cores, Core 0 and 1, which we experimentally determined to be sufficient for accurate and timely SLAM processing—when they run in isolation. Note that the maximum observed per-core CPU utilization of the SLAM threads is less than 70%, meaning there is additional slack that can potentially be used by best-effort tasks.

As for input data for the SLAM task, we use the five Machine Hall (MH) scenarios from the EuRoC dataset [10], MH01-MH05, though we primarily use the MH01 scenario. The image frames from the dataset are fed to the SLAM task through an instance of `rosbag2` [16], which was running on Core 2 with a real-time priority of 2 such that it is not delayed by any best-effort tasks. Note that all MH datasets playback input data at a frequency of 20Hz. The observed CPU utilization of `rosbag2` is about ~5-10% of the Core 2.

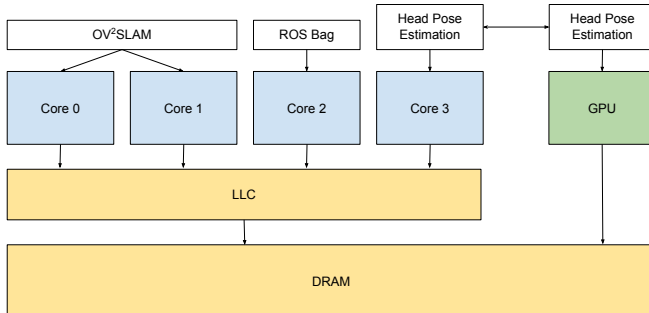


Fig. 1: Tasks to core assignments of the AR-HUD case-study on Jetson Nano.

For the head pose estimation task, we use the HopeNet-Lite DNN model [15], which is a lightweight version of the original HopeNet model [33] and uses the ShuffleNet V2 model [25] as its backbone. Note that the HopeNet-Lite is mainly processed on the GPU but a single CPU core (Core 3) is also used to launch the GPU kernel and monitor its progress. The HopeNet-Lite model could process input frames at about ~35 ms per frame when running in isolation on the Jetson Nano platform. We configure the task to run periodically at the same 20Hz rate as the SLAM task and assign it a real-time priority of 1 as the task is determined to be a *non-critical, high priority task* [3]. In addition, we pin the HopeNet-Lite task to a CPU core distinct from the SLAM task cores, Core 3, so that none of its required CPU operations (e.g. CUDA kernel launch, etc.) are interfered with by the OV<sup>2</sup>SLAM threads.

Figure 1 gives a visual representation of the setup we use and how we assign the AR-HUD tasks to CPU cores on the target platform.

Task	Thread	Core(s)	Real-Time Priority	Rate (Hz)
OV <sup>2</sup> SLAM	Front-End	0,1	2	20
	Mapping			-
	State Optimization			-
ROS bag	-	2	2	20
Head Pose Est.	-	3,GPU	1	20

TABLE II: Real-time tasks/threads/core mapping and scheduling parameters in the AR-HUD case study. Note that all real-time tasks are scheduled using the SCHED\_FIFO real-time scheduler.

Table II then shows the real-time characteristics for all of the tasks and threads we utilize in the AR-HUD case study.

### C. Operating System Setup

For the operating system we run Ubuntu 18.04 with Linux kernel 4.9, which is patched with PALLOC [43] to support LLC partitioning. PALLOC exploits virtual memory page translations to enforce page allocations to specific page colors. With PALLOC, we partition the LLC into four equally sized partitions (colors) and perform a 2/2 split of those partitions. Namely, the OV<sup>2</sup>SLAM algorithm gets two LLC partitions, and all other tasks share the remaining two cache partitions. Note that all best-effort tasks—those that are scheduled using Linux’s default CFS scheduler—also share the latter two cache partitions in order to minimize any performance impact to the SLAM task, which is real-time critical. Note that, in PALLOC, tasks—not cores—can be mapped to any cache partitions.

## V. ANALYZING THE EFFECTS OF SHARED RESOURCE CONTENTION

In this section, we evaluate the impact of shared resource contention on the performance of the OV<sup>2</sup>SLAM algorithm.

### A. Impact of Co-scheduling DoS Attacks

In this experiment we evaluate the impacts of DoS attack co-runners and whether they are effective in degrading

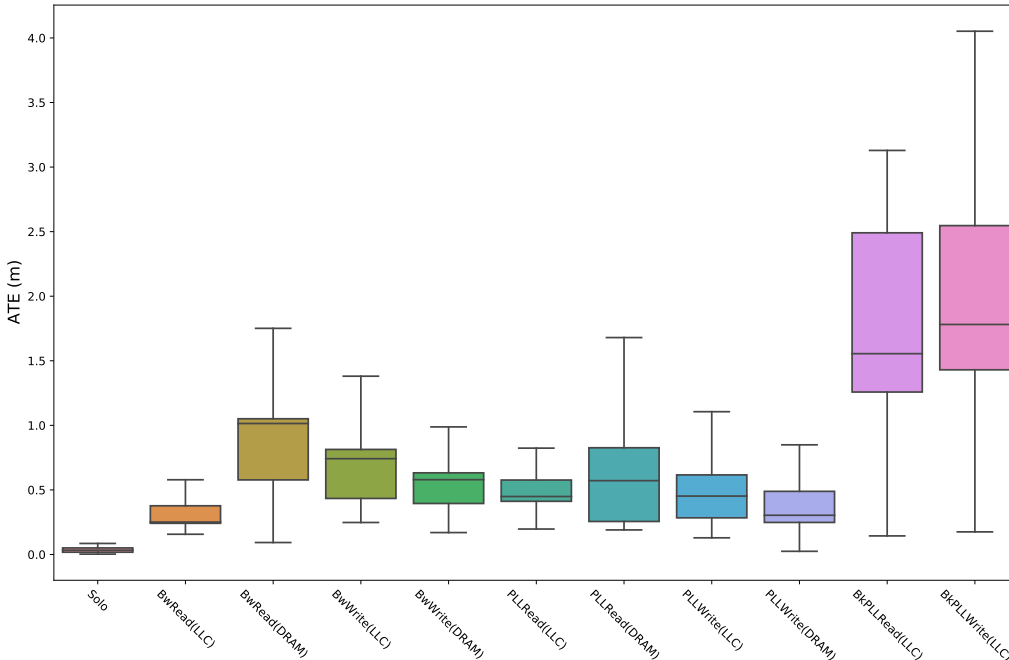


Fig. 2: Impact of DoS attacks on the Absolute Trajectory Error (ATE) of the OV<sup>2</sup>SLAM generated trajectory.

OV<sup>2</sup>SLAM performance in a given scenario. Note that we did not execute the HopeNet-Lite DNN task in this experiment in order to focus on SLAM performance and its sensitivity to DoS attacks.

The experiment setup is as follows: We first run an instance of the OV<sup>2</sup>SLAM task using the MH01 scenario in the EuRoC dataset [10]. Once finished, we calculate the algorithm’s *Absolute Trajectory Error (ATE)* relative to the known ground-truth trajectory [10]. We then repeat the experiment but with instances of a DoS attacker on all four available cores. We again calculate the ATE and compare it to the solo case to determine whether the attackers had any noticeable impact.

Note that we run the DoS attacks as best-effort tasks while run the OV<sup>2</sup>SLAM task as a real-time task. Because Linux strictly prioritizes real-time tasks over best-effort ones, the DoS attack tasks can only be executed on cores which are not executing any of the RT tasks. In other words, whenever the threads of the SLAM task become ready, they immediately preempt any DoS attacker tasks. Note also that, as mentioned earlier, the DoS attack tasks are assigned to a separate LLC cache partition from the SLAM task, which further minimizes any negative effect of co-scheduling.

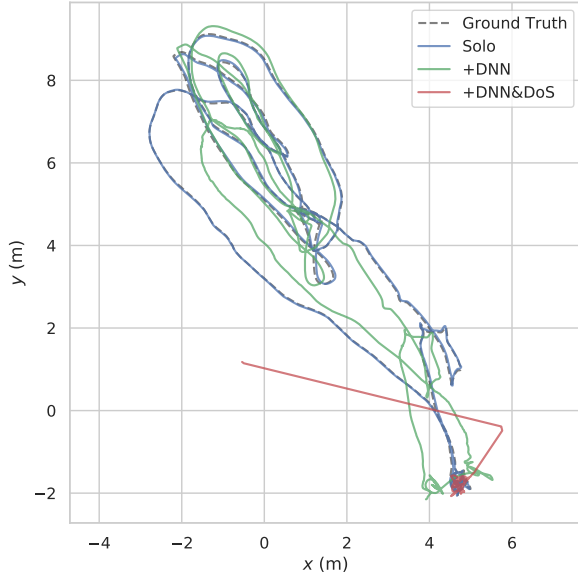
Figure 2 shows a boxplot of the OV<sup>2</sup>SLAM ATE, collected over the entire duration of the MH01 dataset, both alone and alongside each of the tested DoS attacks (X-axis). First and foremost, we find that all of the tested DoS attacks cause significant negative impacts to the tracking performance (measured in ATE), despite the fact that they cannot preempt the real-time SLAM task running on the same cores. This is because the use of real-time scheduling does not prevent shared resource contention caused by the DoS attackers run-

ning on different cores. Note that, for this scenario, ATEs of  $\sim 0.3$  or more means significant deviations from the ground truth, which could potentially cause system failure (e.g., a crash) in the real-world [23]. Moreover, we find that the recently proposed cache bank-aware DoS attacks [7]—denoted as *BkPLLRead(LLC)* and *BkPLLWrite(LLC)* for read and write, respectively—are by far the most effective in terms of ATE increase. Concretely, the *BkPLLRead(LLC)* attack increased the median ATE to  $>1.7$  ( $\sim 49X$  increase over solo) and the *BkPLLWrite(LLC)* attack increased it to  $>1.9$  ( $\sim 55X$  increase). In other words, these attacks caused the OV<sup>2</sup>SLAM algorithm’s detected trajectory to deviate from the ground truth trajectory by close to two meters on average, and more than four meters in the worst-case.

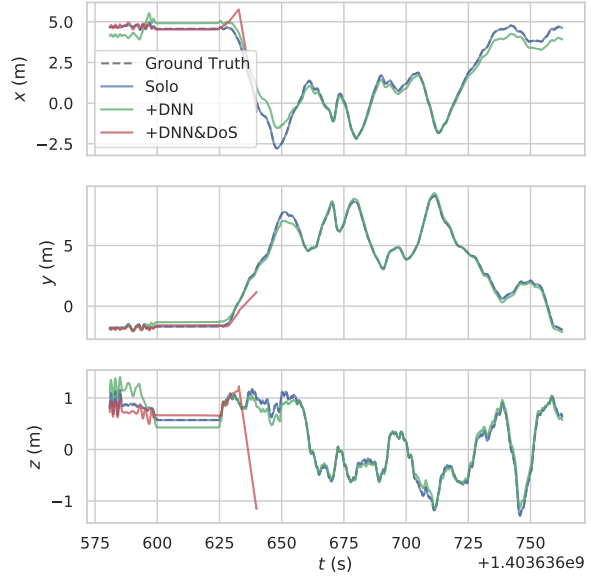
### B. Impact of Co-scheduling HopeNet-Lite on Integrated GPU

In this experiment, we evaluate the impact of co-scheduling the HopeNet-Lite head pose estimator on the performance of the OV<sup>2</sup>SLAM task. We compare the following configurations: (1) *+DNN* in which HopeNet-Lite is co-scheduled with OV<sup>2</sup>SLAM; and (2) *+DNN&DoS* in which both HopeNet-Lite and the DoS attack tasks are co-scheduled with OV<sup>2</sup>SLAM. Note that the DoS attackers are best-effort tasks while both OV<sup>2</sup>SLAM and HopeNet-Lite are real-time tasks. As per the results in the previous subsection, we use the *BkPLLWrite(LLC)* attack for the aggressor workloads as it was the most effective at degrading the performance of the SLAM task.

Figure 3 shows the generated trajectories for both the *+DNN* and *+DNN&DoS* cases. First, the addition of the HopeNet-Lite task significantly impacts the accuracy of OV<sup>2</sup>SLAM with the median ATE increasing to  $>0.8$ , which can be seen by



(a) Trajectory in XY plane



(b) X, Y and Z positions over time

Fig. 3: OV<sup>2</sup>SLAM trajectory when run alongside both *BkPLLWrite(LLC)* DoS attackers and a GPU-based DNN application.

how the trajectory deviates from the ground truth. However, when HopeNet-Lite is combined with the DoS attacks, in *+DNN&DoS*, OV<sup>2</sup>SLAM suffers a drastic performance degradation to the point that it completely fails to generate a full trajectory. This is because OV<sup>2</sup>SLAM is unable to keep up with the input data—due to shared resource contention—and ends up dropping a majority of the frames. Our analysis shows that only  $\sim 26\%$  of the input image frames were processed in *+DNN&DoS*, as opposed to more than  $>97\%$  in either the *+DNN* or *+DoS* cases.

### C. Runtime Analysis of OV<sup>2</sup>SLAM and HopeNet-Lite

To further investigate the impacts of shared resource contention on the AR-HUD application, we perform a detailed execution time analysis on the three CPU threads of the OV<sup>2</sup>SLAM task—the *Front End*, *Mapping* and *State Optimization* threads—and the DNN-based head pose estimator HopeNet-Lite. For the OV<sup>2</sup>SLAM threads, we measure and record the execution times of each thread when they perform their main computational loop (e.g. *Front End* receives a new input frames, *Mapping* receives a new keyframe, etc.). For the DNN task, we measure its inference times across 1000 input frames. We then compute the distribution of execution times for all tasks and threads to determine whether any of them experience execution delays due to co-runner interference. For the OV<sup>2</sup>SLAM analysis, we re-run three of the test scenarios previously performed: the *Solo* case where it runs alone, the *+DoS* case alongside *BkPLLWrite(LLC)* DoS attack, and the *+DNN* case alongside the HopeNet-Lite task. For the HopeNet-Lite task, we also measure its inference times in three different scenarios: *Solo* when it runs alone, *+SLAM*

when run with the SLAM task, and *+SLAM&DoS* when run with both the SLAM task and *BkPLLWrite(LLC)* DoS attack.

Figure 4 shows the execution time distributions for all real-time tasks and threads in each of their respective scenarios. For the OV<sup>2</sup>SLAM task, we observe execution time increases in all three threads when adversarial co-runners were present. Notably, though, we find that the *Front End* and *Mapping* threads see greater WCET slowdowns from the DNN co-runner than they do the DoS attacks. On the other hand, the *State Optimization* thread is much more impacted by the DoS attacks in terms of the observed WCET. Given the disparity in SLAM ATE loss between the DoS attackers (55X) and the DNN co-runner (27X), we find that *State Optimization* is of greater importance for OV<sup>2</sup>SLAM in generating more accurate trajectories, which is consistent with prior findings [23].

Lastly, Figure 4d shows the time distributions for the HopeNet-Lite task. Similar to the SLAM task, the HopeNet-Lite task is also slowed down when the two are run together (on different cores/GPU), going from an average inference time of  $\sim 34$  ms alone to  $\sim 37$  ms alongside the SLAM task. When the DoS attacks are then added, the average inference time increases again to  $\sim 48$  ms.

## VI. MITIGATING SHARED RESOURCE CONTENTION

In this section, we present a mitigation solution to protect the real-time AR-HUD application in the presence of aggressor tasks (i.e., DoS attacks).

### A. RT-Gang++

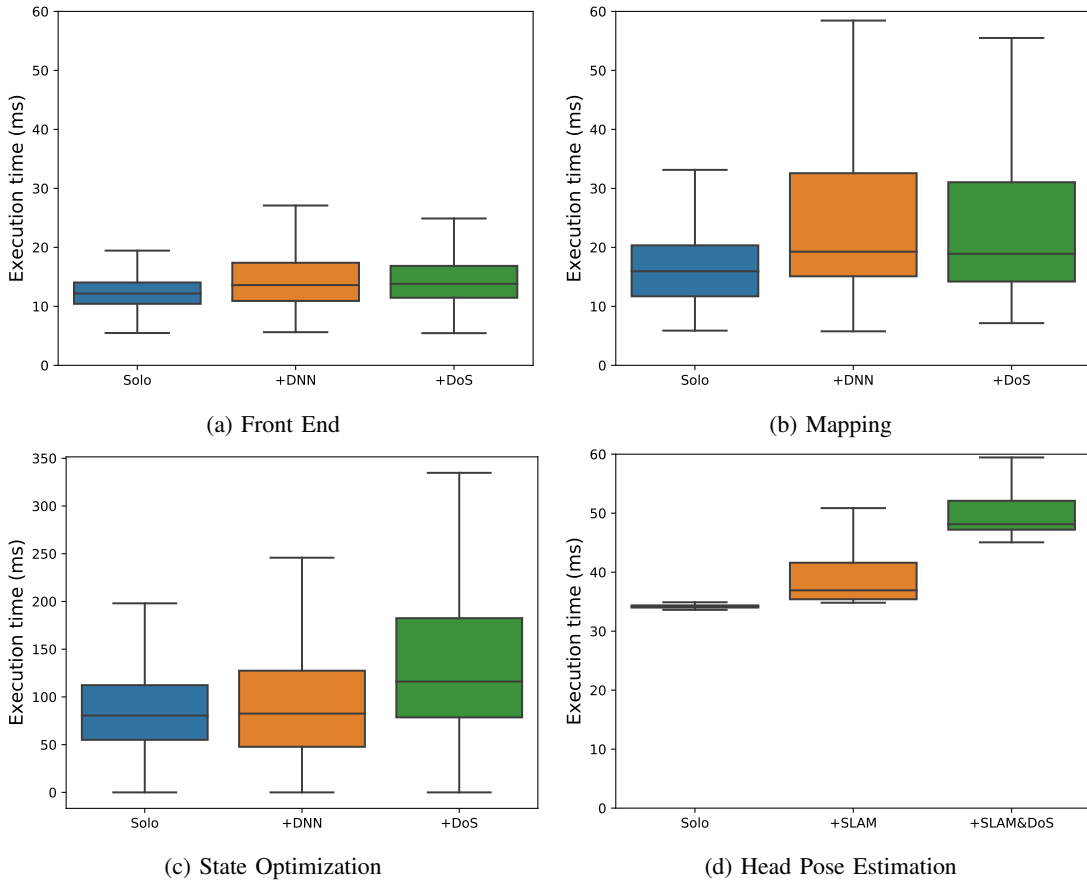


Fig. 4: Execution time distributions of all real-time AR-HUD tasks and threads.

In this work, we leverage the RT-Gang scheduling framework [2], a real-time gang scheduler that is implemented as an extension to the existing real-time task scheduler in the Linux kernel. RT-Gang supports a simple real-time gang scheduling policy, which allows only one parallel real-time gang at a time across all cores. Moreover, RT-Gang supports memory bandwidth throttling of best-effort tasks to protect any currently running real-time gang task. In other words, RT-Gang throttles any cores that execute best-effort tasks whenever a real-time gang task is running on any cores in the system. On the other hand, if no real-time gang is scheduled on the system, then the best-effort tasks have full access to the memory bandwidth.

When we tried to apply RT-Gang to mitigate the shared resource contention problem in the AR-HUD application of the ARM industrial challenge, however, we encountered the following challenges. First, the original RT-Gang supports only a single gang task at a time. While multiple tasks can be grouped together to form a “virtual gang” task [1], it is only applicable when all tasks of the virtual gang have the same period and the same real-time priority. As described in Table II, however, one of the three real-time tasks, the DNN task, in our case study has a lower real-time priority than the other two real-time tasks. Second, when we use the cache

bank-aware DoS attack [7] as the best-effort aggressor tasks, RT-Gang’s memory bandwidth throttling capability becomes ineffective in protecting the RT tasks because the aggressors do not consume any memory bandwidth as they target LLC bank contention instead. Lastly, RT-Gang does not offer any contention mitigation mechanisms between the real-time tasks. This means that there is no way to minimize negative performance impact on a higher priority OV2SLAM task due to co-scheduling the lower priority DNN real-time task, which runs on the iGPU.

To address the challenges, we make three *extensions* to the vanilla RT-Gang: (1) We add support for a partitioned real-time gang scheduling capability; (2) We add support for iGPU bandwidth throttling; (3) We add support for LLC bandwidth throttling. We call the resulting system *RT-Gang++*.

### B. Partitioned Gang Scheduling

One major feature of the baseline RT-Gang is that it allows only one real-time gang task at a time across the all cores in a multicore CPU. While it does prevent shared resource contention between RT tasks by design, which is desirable for predictability, it is also a limitation in terms of scalability because not all tasks can benefit from a large number of cores and the number of cores in CPUs keeps increasing. While RT-Gang somewhat mitigates the problem by supporting so

called “virtual gangs”, which is a collection of multiple real-time tasks with the same period and the same priority that collectively acts like a single gang task, it cannot be used when either the priority or the period of any RT task differs from the rest. Moreover, many modern multicore CPUs are often composed of multiple clusters, each of which may have different set computing and memory resources that are not shared with the rest. For example, many ARM multicore CPUs incorporate the big.LITTLE architecture where one cluster is composed of powerful “big” cores and the other cluster is composed of efficient “little” cores. Not only do the clusters have different types of CPU cores, but they also often have cluster-private shared resources that are not shared across the clusters, which reduces the need to strictly adhere to the one-gang-task-at-a-time policy of RT-Gang.

In RT-Gang++, we support multiple *partitions* where each partition is composed of a statically determined set of cores. The one-gang-task-at-a-time is then applied to each partition rather than being applied globally. This means that multiple gang tasks, each with different priority and/or period, can run simultaneously as long as they are assigned to different partitions. For our AR-HUD case-study in Table II, we assign OV<sup>2</sup>SLAM and EuRoC playback tasks to form a virtual gang task and assign it into a gang partition, which is comprised of core 0, 1, and 2, while assigning the DNN task (head pose estimation) on another gang partition, which is composed of the core 3 and the iGPU. In this way, the system can run two active gang tasks with different priority and period simultaneously.

### C. iGPU Memory Bandwidth Throttling

When multiple real-time tasks run together, however, they inevitably contend on the shared resources. As observed in Section V-B, co-scheduling the DNN task in particular has detrimental effect to the more critical OV<sup>2</sup>SLAM task’s accuracy. The baseline RT-Gang, unfortunately, does not provide any means to address the contention between the two co-scheduled RT tasks. In this work, we leverage hardware-level GPU bandwidth throttling capability of the platform we used for evaluation. Specifically, the Tegra X1 SoC of the Jetson Nano platform supports a number of QoS features at its memory controller, one of which is hardware-level throttling of subsets of hardware components that access the memory controller [30]. The throttling feature of the memory controller provides 32 programmable throttling levels that can be applied to throttle the integrated GPU, which we used to throttle the DNN task whose memory access from the GPU impacts the performance of the OV<sup>2</sup>SLAM task.

Figure 5 shows the average HopeNet-Lite inference latencies under each of the 32 throttling levels when running alone in isolation. Note that GPU throttling does not impact the performance of the DNN task until the throttling level reaches around 15, indicating that sufficient bandwidth is provided until that point. After that, more aggressive throttling does impact the performance of the DNN. When the throttling level is 31, which is the maximum, the average inference latency

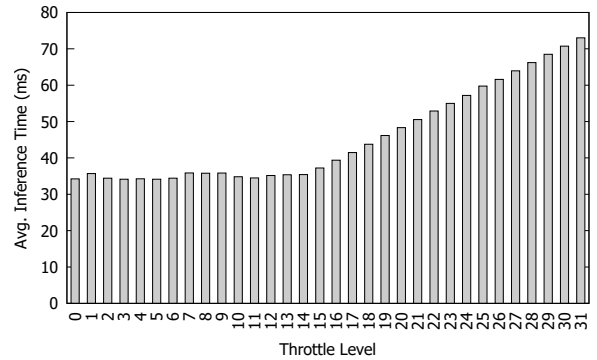


Fig. 5: Impact of GPU throttling on HopeNet-Lite DNN.

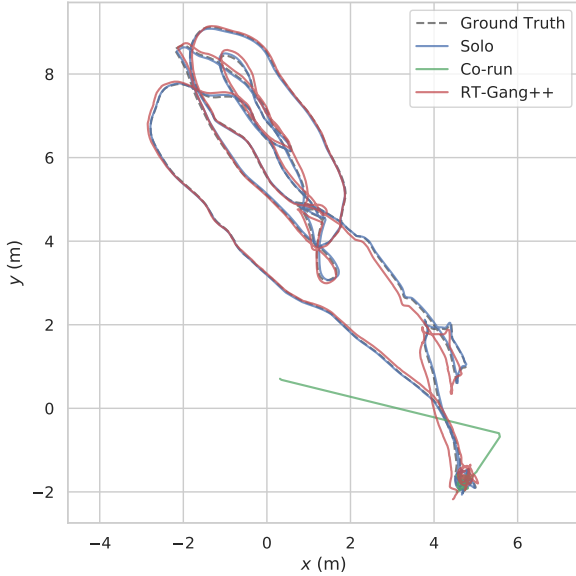
is increased to  $\sim 73$  ms, which is about twice longer than without throttling. Note that there is a tradeoff between the accuracy of the SLAM task and the latency of the DNN task as more aggressive throttling of the GPU, which is used by the latter, will be helpful to achieve higher accuracy (lower ATE) for the SLAM task but it will increase the latency of the DNN task. As such, finding a “sweet spot” for the target application is necessary. For our study, we experimentally chose the level 20 as it was the maximum throttling level that still can provide 20Hz real-time performance for the DNN inference task. However, one can choose a more aggressive throttling level (e.g., the level 31) if achieving the highest accuracy of the SLAM task is more important than processing the DNN task at 20Hz. In our testing, using the GPU throttling level 31 allows the SLAM task to achieve near perfect isolation but at the cost of doubling the latency of the DNN task.

### D. LLC Bandwidth Throttling

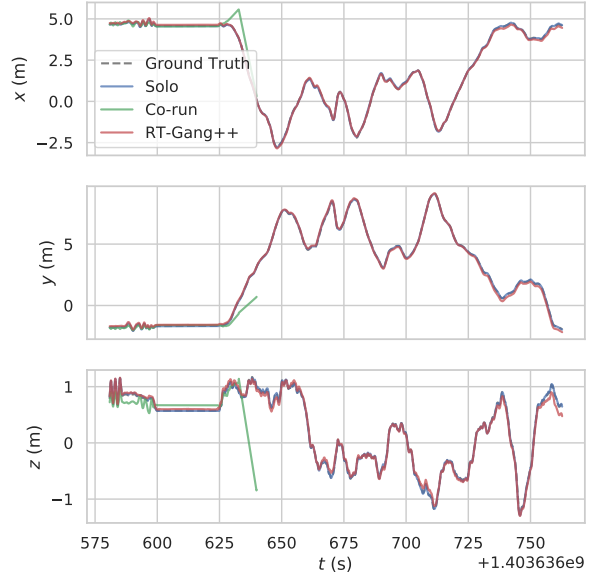
For our case-study application, both the OV<sup>2</sup>SLAM and DNN real-time tasks must be protected from the interference of co-scheduled aggressor tasks, which are scheduled in a best-effort manner (i.e., scheduled on any cores that do not execute RT tasks). As discussed in Section V-A, when DoS attackers are used as the aggressor tasks, the performance of the OV<sup>2</sup>SLAM algorithm is significantly reduced even though the DoS attackers cannot preempt the SLAM task due to shared resource contention. In particular, we find that cache bank-aware DoS attack [7] is particularly effective in negatively impacting accuracy of the SLAM task. Unfortunately, however, the baseline RT-Gang’s memory bandwidth throttling capability does not provide any protection against the cache-bank DoS attack, as it generates LLC cache hits and does not consume any memory bandwidth.

In RT-Gang++, we add support for LLC bandwidth throttling capability by utilizing the L1-D cache miss performance counter (L1D\_CACHE\_REFILL) of the CPU cores to track and throttle LLC (L2) bandwidth used by the best-effort DoS attacker tasks. Note that we use an experimentally determined LLC bandwidth threshold of 100 MB/s when LLC throttling is enabled.





(a) Trajectory in X-Y plane



(b) X, Y, and Z positions over time.

Fig. 6: Impact of RT-Gang++ on OV<sup>2</sup>SLAM performance.

### E. Evaluation Results

In this subsection, we evaluate the performance of RT-Gang++. The basic experiment setup is the same as those in Section IV: i.e., we execute the SLAM task on Cores 0 and 1, the EuRoC dataset playback task on Core 2, and the DNN task on Core 3 and the iGPU. We repeat the experiment without and with RT-Gang++, denoted as *Co-run* and *RT-Gang++*, respectively.

Figure 6 shows the trajectory generated by the OV<sup>2</sup>SLAM task, and the X, Y and Z positions of the trajectory over time. Compared to *Co-run* case, where OV<sup>2</sup>SLAM could only create a highly inaccurate partial trajectory, RT-Gang++ effectively protects against the *BkPLLWrite(LLC)* attackers such that OV<sup>2</sup>SLAM can produce a trajectory that is significantly closer to the ground truth.

To determine RT-Gang++’s impact to best-effort tasks, we also measure the performance of the *BkPLLWrite(LLC)* attackers both with and without RT-Gang++ enabled. For this, we again run the *Co-run* and *RT-Gang++* cases but measure the LLC bandwidth consumed by the DoS attacks in both scenarios.

Core	Solo	Co-run	RT-Gang++
0	8241	2413	956
1	8470	1304	792
2	7643	5628	1211
3	7496	156	119

TABLE III: LLC bandwidth consumed by all best-effort *BkPLLWrite(LLC)* attackers. All values are in MB/s.

Table III shows the best-effort bandwidth measured for each core. First, we find that the cores achieve the highest

Test Case	Avg. Inference Time (ms)
Solo	34.23
Co-run	36.32
RT-Gang++	48.69

TABLE IV: Average inference latency of the DNN task

bandwidths when LLC throttling is not enabled. Then, when LLC throttling is enabled in the RT-Gang++ framework (i.e. dynamic throttling), the best-effort tasks can still achieve decent bandwidths as they are allowed full access to the LLC during slacks between real-time tasks.

Likewise, we also measure RT-Gang++’s impact to the head pose estimation DNN task. Table IV shows the average inference times achieved by the DNN task across the different test cases. In the *Co-run* case, we found that the DNN task’s inference time was slightly impacted, going from  $\sim 34$  to  $\sim 36$  ms on average but that it could still meet the 50 ms deadline with ease. Similarly, with RT-Gang++ and iGPU bandwidth throttling enabled, we found that the DNN task’s inference time was further increased to  $\sim 49$  ms on average, meaning that it could still achieve 20 Hz performance on average.

Finally, to further test RT-Gang++, we run the OV<sup>2</sup>SLAM task on the other four machine hall EuRoC scenarios, MH02-MH05.

Table V then shows the median ATE values for the trajectories generated by OV<sup>2</sup>SLAM. Even with RT-Gang++ enabled, we still see notable performance drops when iGPU bandwidth throttling is not enabled. On the other hand, when both LLC and iGPU bandwidth throttling are enabled, we see significant improvements to ATE performance such that they are with relative margin on the *Solo* case ATEs. Note that an ATE value

Dataset	Solo	RT-Gang++ (No iGPU throttling)	RT-Gang++
MH01	0.03	0.36	0.11
MH02	0.04	0.47	0.07
MH03	0.08	0.24	0.20
MH04	0.15	2.86	0.29
MH05	0.12	0.80	0.23

TABLE V: OV<sup>2</sup>SLAM median ATE on the Machine Hall scenarios from the EuRoC dataset. Note that *Co-run* is not included as it fails to generate full trajectory due to contention.

less than 0.3 is desirable for these scenarios [23], which we were able to satisfy in all cases with RT-Gang++ fully enabled.

## VII. RELATED WORK

Simultaneous Localization and Mapping (SLAM) algorithms are at the heart of many robotics applications, including ADAS and self-driving systems, as they are used to localize the position and pose of the ego-vehicle in connection with the surrounding environment. Due to the relatively cheaper cost of camera sensors, many efforts have been made towards solving the challenge of Visual SLAM. The PTAM algorithm was the first to introduce a multi-threaded Visual SLAM implementation [22] for improved real-time performance. It separated tracking and mapping into separate parallel threads on a dual-core processor, which allowed them to create more detailed 3D maps and achieve state-of-the-art accuracy. This type of multi-threaded approach has since been widely adopted in many Visual SLAM implementations. Notable examples of this include the LSD-SLAM algorithm [12], the many iterations of the ORB-SLAM algorithm [28], [29], [11], and the OV<sup>2</sup>SLAM algorithm [14], which was used in this paper. These algorithms detect features of the camera images and track the features to locate their positions in the world. Recently, Li et. al, observed that performance of SLAM algorithms can be sensitive to execution timing delays and proposed an adaptive strategy within the SLAM to minimize performance degradation [23]. In contrast, our work propose a system-level solution that does not require changes in the SLAM algorithm and provides in-depth microarchitectural analysis on resource contention.

Microarchitectural DoS attacks are software attacks specifically designed to induce a high-degree of resource contention. DoS attacks on several shared resources have been studied and evaluated. Moscibroda et al. proposed a DoS attack that targets a FR-FCFS scheduling algorithm [31] in shared DRAM controllers [27]. Keramidas et al. demonstrated DoS attacks targeting shared LLC space and, to address them, proposed a cache replacement policy that gave the attackers access to less of the LLC space [19]. Woo et al. investigated DoS attacks on bus bandwidth and shared cache space in a simulated environment [39]. Valsan et al. and Bechtel et al. showed that DoS attacks could target internal LLC hardware structures [9], [8], [38]. Based on [9], Iorga et al. presented a statistical approach for testing DoS attacks [18]. Li et al. applied machine learning to better optimize DoS attackers, resulting in WCET slowdowns >400X [24]. GPU-based DoS attacks have also

been studied by researchers. Yandrofski et al, systematically studied shared resource contention on discrete Nvidia GPUs by generating various adversarial programs [41]. Bechtel et al., implemented DoS attacks targeted towards Intel iGPUs, as they also access the LLC.

Much effort has been devoted to address the problem of shared resource contention in multicore in the real-time systems research community. Partitioning of shared resources, especially shared cache [26], [20], [42], [21], [13], [40], [32] and DRAM banks [21], [13], has been extensively studied. Bandwidth throttling [44], [40], [37], [34], [35], [46] has been another popular approach. For example, MemGuard [44] uses per-core hardware performance counters to throttle each core’s bandwidth usage, which has been a standard throttling technique in many subsequent studies. Recently, both Intel and ARM also introduced hardware support for shared resource partitioning and throttling [17], [5], though their effectiveness in providing isolation for real-time systems is still insufficient [45], [36], [7]. In most of these works, cores are partitioned between RT and best-effort cores. For example, Saeed et al. proposed a resource management system that reserves a single core as the RT core and dynamically throttles memory bandwidth usage of the other best-effort cores to bound their interference on the RT core [34], [35]. However, such an approach can significantly under utilize computing resources. Likewise, for applications like the AR-HUD in the industrial challenge problem one core is not sufficient, meaning they would be unable to run due to a lack of computing capacity. RT-Gang [2], [1] offers more flexible scheduling potential as all cores can be utilized for both RT and best-effort tasks. This is because the OS automatically throttles the best-effort tasks only when a RT task is running on any core(s) in the multicore system. In this work, we leverage RT-Gang but address its limitations by adding GPU throttling, dynamic cache bandwidth throttling, and partitioned gang scheduling.

## VIII. CONCLUSION

In this paper, we presented a solution to the Industrial Challenge problem put forth by ARM in 2022 [3]. We systematically analyzed the effect of shared resource contention to an augmented reality head-up display (AR-HUD) case-study application of the industrial challenge on a heterogeneous multicore platform. Using micro-architectural denial-of-service (DoS) attacks as aggressor tasks of the challenge, we showed that such aggressors can dramatically impact the latency and accuracy of the AR-HUD application, which could result in significant deviations of the estimated trajectories from the ground truth, despite the best effort to mitigate their influence by using cache partitioning and real-time scheduling of the AR-HUD application. To address this we propose RT-Gang++, which combines LLC and iGPU bandwidth throttling to mitigate shared resource contention from their respective resources. By deploying RT-Gang++, we were able to effectively protect the performance of the critical SLAM task, such that

it could achieve near solo case performance, without having to over-provision the system.

For future work, we plan to perform similar case studies on more capable platforms than the Jetson Nano, such as the Jetson Xavier or Jetson Orin lines of embedded platforms, to evaluate their susceptibility to shared resource contention and the generality of the proposed RT-Gang++ framework.

## REFERENCES

- [1] W. Ali, R. Pellizzoni, and H. Yun. Virtual gang scheduling of parallel real-time tasks. In *Design, Automation & Test in Europe Conference & Exhibition (DATE)*, pages 270–275. IEEE, 2021.
- [2] W. Ali and H. Yun. RT-Gang: Real-Time Gang Scheduling Framework for Safety-Critical Systems. In *RTAS*, 2019.
- [3] M. Andreozzi, G. Gabrielli, B. Venu, and G. Travaglini. Industrial Challenge 2022: A High-Performance Real-Time Case Study on Arm. In *ECRTS*, 2022.
- [4] SOAFEE. <https://www.soafee.io/>.
- [5] ARM. *Arm Architecture Reference Manual Supplement: Memory System Resource Partitioning and Monitoring (MPAM)*, DDI-0598B.b, 2020.
- [6] M. Bechtel and H. Yun. Memory-Aware Denial-of-Service Attacks on Shared Cache in Multicore Real-Time Systems. *Transactions on Computers*, 2021.
- [7] M. Bechtel and H. Yun. Cache Bank-Aware Denial-of-Service Attacks on Multicore ARM Processors. In *RTAS*, 2023.
- [8] M. G. Bechtel, E. McElhiney, M. Kim, and H. Yun. DeepPicar: A Low-cost Deep Neural Network-based Autonomous Car. In *RTCSA*, 2018.
- [9] M. G. Bechtel and H. Yun. Denial-of-Service Attacks on Shared Cache in Multicore: Analysis and Prevention. In *RTAS*, 2019.
- [10] M. Burri, J. Nikolic, P. Gohl, T. Schneider, J. Rehder, S. Omari, M. W. Achtelik, and R. Siegwart. The EuRoC Micro Aerial Vehicle Datasets. *The International Journal of Robotics Research*, 2016.
- [11] C. Campos, R. Elvira, J. J. G. Rodríguez, J. M. Montiel, and J. D. Tardós. Orb-slam3: An accurate open-source library for visual, visual-inertial, and multimap slam. *IEEE Transactions on Robotics*, 2021.
- [12] J. Engel, T. Schöps, and D. Cremers. LSD-SLAM: Large-Scale Direct Monocular SLAM. In *ECCV*, 2014.
- [13] F. Farshchi, P. K. Valsan, R. Mancuso, and H. Yun. Deterministic Memory Abstraction and Supporting Multicore System Architecture. In *ECRTS*, 2018.
- [14] M. Ferrera, A. Eudes, J. Moras, M. Sanfourche, and G. Le Besnerais. OV<sup>2</sup>SLAM: A Fully Online and Versatile Visual SLAM for Real-Time Applications. *IEEE robotics and automation letters*, 2021.
- [15] HopeNet-Lite. <https://github.com/OverEuro/deep-head-pose-lite>.
- [16] rosbag2. <https://github.com/ros2/rosbag2>.
- [17] Intel. Intel® Resource Director Technology (Intel® RDT) Framework. <https://www.intel.com/content/www/us/en/architecture-and-technology/resource-director-technology.html>.
- [18] D. Iorga, T. Sorensen, J. Wickerson, and A. F. Donaldson. Slow and Steady: Measuring and Tuning Multicore Interference. In *RTAS*, 2020.
- [19] G. Keramidas, P. Petoumenos, S. Kaxiras, A. Antonopoulos, and D. Serpanos. Preventing denial-of-service attacks in shared cmp caches. In *SAMOS*, 2006.
- [20] H. Kim, A. Kandhalu, and R. Rajkumar. A Coordinated Approach for Practical OS-Level Cache Management in Multi-core Real-Time Systems. In *ECRTS*, 2013.
- [21] N. Kim, B. C. Ward, M. Chisholm, J. H. Anderson, and F. D. Smith. Attacking the One-Out-of-M Multicore Problem by Combining Hardware Management with Mixed-Criticality Provisioning. *Real-Time Systems*, 2017.
- [22] G. Klein and D. Murray. Parallel Tracking and Mapping for Small AR Workspaces. In *ISMAR*, 2007.
- [23] A. Li, H. Liu, J. Wang, and N. Zhang. From Timing Variations to Performance Degradation: Understanding and Mitigating the Impact of Software Execution Timing in SLAM. In *IROS*, 2022.
- [24] A. Li, M. Sudvarg, H. Liu, Z. Yu, C. Gill, and N. Zhang. PolyRhythm: Adaptive Tuning of a Multi-Channel Attack Template for Timing Interference. In *RTSS*, 2022.
- [25] N. Ma, X. Zhang, H.-T. Zheng, and J. Sun. Shufflenet V2: Practical Guidelines for Efficient CNN Architecture Design. In *ECCV*, 2018.
- [26] R. Mancuso, R. Dudko, E. Betti, M. Cesati, M. Caccamo, and R. Pellizzoni. Real-Time Cache Management Framework for Multi-core Architectures. In *RTAS*, 2013.
- [27] T. Moscibroda and O. Mutlu. Memory Performance Attacks: Denial of Memory Service in Multi-Core Systems. In *USENIX Security Symposium*, 2007.
- [28] R. Mur-Artal, J. M. M. Montiel, and J. D. Tardós. ORB-SLAM: A Versatile and Accurate Monocular SLAM System. *IEEE transactions on robotics*, 2015.
- [29] R. Mur-Artal and J. D. Tardós. ORB-SLAM2: An Open-Source SLAM System for Monocular, Stereo, and RGB-D Cameras. *IEEE transactions on robotics*, 2017.
- [30] NVIDIA. *Tegra X1 Mobile Processor technical reference manual (revision 1.3p)*, 2019.
- [31] S. Rixner, W. J. Dally, U. J. Kapasi, P. Mattson, and J. Owens. Memory Access Scheduling. In *ACM SIGARCH Computer Architecture News*, 2000.
- [32] S. Roozkhosh and R. Mancuso. The Potential of Programmable Logic in the Middle: Cache Bleaching. In *RTAS*, 2020.
- [33] N. Ruiz, E. Chong, and J. M. Rehg. Fine-Grained Head Pose Estimation Without Keypoints. In *CVPR*, 2018.
- [34] A. Saeed, D. Dasari, D. Ziegenbein, V. Rajasekaran, F. Rehm, M. Pressler, A. Hamann, D. Mueller-Gritschneider, A. Gerstlauer, and U. Schlichtmann. Memory Utilization-Based Dynamic Bandwidth Regulation for Temporal Isolation in Multi-Cores. In *RTAS*, 2022.
- [35] A. Saeed, D. Hoornaert, D. Dasari, D. Ziegenbein, D. Mueller-Gritschneider, U. Schlichtmann, A. Gerstlauer, and R. Mancuso. Memory latency distribution-driven regulation for temporal isolation in mpsocs. In *Euromicro Conference on Real-Time Systems (ECRTS)*. Schloss Dagstuhl-Leibniz-Zentrum für Informatik, 2023.
- [36] P. Sohal, M. Bechtel, R. Mancuso, H. Yun, and O. Krieger. A Closer Look at Intel Resource Director Technology (RDT). In *RTNS*, pages 127–139, 2022.
- [37] P. Sohal, R. Tabish, U. Drepper, and R. Mancuso. E-WarP: a System-wide Framework for Memory Bandwidth Profiling and Management. In *RTSS*, 2020.
- [38] P. K. Valsan, H. Yun, and F. Farshchi. Taming Non-blocking Caches to Improve Isolation in Multicore Real-Time Systems. In *RTAS*, 2016.
- [39] D. H. Woo and H. Lee. Analyzing performance vulnerability due to resource denial of service attack on chip multiprocessors. In *CMP-MSI*, 2007.
- [40] M. Xu, L. T. X. Phan, H.-Y. Choi, Y. Lin, H. Li, C. Lu, and I. Lee. Holistic Resource Allocation for Multicore Real-Time Systems. In *RTAS*, 2019.
- [41] T. Yandrofski, J. Chen, N. Otterness, J. H. Anderson, and F. Smith. Making Powerful Enemies on NVIDIA GPUs. In *RTSS*, 2022.
- [42] Y. Ye, R. West, Z. Cheng, and Y. Li. Coloris: a Dynamic Cache Partitioning System Using Page Coloring. In *PACT*, 2014.
- [43] H. Yun, R. Mancuso, Z.-P. Wu, and R. Pellizzoni. PALLOC: DRAM Bank-Aware Memory Allocator for Performance Isolation on Multicore Platforms. In *RTAS*, 2014.
- [44] H. Yun, G. Yao, R. Pellizzoni, M. Caccamo, and L. Sha. MemGuard: Memory Bandwidth Reservation System for Efficient Performance Isolation in Multi-core Platforms. In *RTAS*, 2013.
- [45] M. Zini, D. Casini, and A. Biondi. Analyzing arm’s mpam from the perspective of time predictability. *IEEE Transactions on Computers*, 72(1):168–182, 2022.
- [46] A. Zuepke, A. Bastoni, W. Chen, M. Caccamo, and R. Mancuso. MemPol: Policing Core Memory Bandwidth from Outside of the Cores. In *RTAS*, 2023.